

This is a repository copy of *Regional biomechanical and histological characterisation of the passive porcine urinary bladder: Implications for augmentation and tissue engineering strategies*.

White Rose Research Online URL for this paper:

<https://eprints.whiterose.ac.uk/5234/>

---

## Article:

Korossis, Sotirios, Bolland, Fiona, Southgate, Jenny orcid.org/0000-0002-0135-480X et al. (2 more authors) (2009) Regional biomechanical and histological characterisation of the passive porcine urinary bladder: Implications for augmentation and tissue engineering strategies. *Biomaterials*. pp. 266-275. ISSN 0142-9612

<https://doi.org/10.1016/j.biomaterials.2008.09.034>

---

## Reuse

Items deposited in White Rose Research Online are protected by copyright, with all rights reserved unless indicated otherwise. They may be downloaded and/or printed for private study, or other acts as permitted by national copyright laws. The publisher or other rights holders may allow further reproduction and re-use of the full text version. This is indicated by the licence information on the White Rose Research Online record for the item.

## Takedown

If you consider content in White Rose Research Online to be in breach of UK law, please notify us by emailing [eprints@whiterose.ac.uk](mailto:eprints@whiterose.ac.uk) including the URL of the record and the reason for the withdrawal request.

*promoting access to White Rose research papers*



**Universities of Leeds, Sheffield and York**  
**<http://eprints.whiterose.ac.uk/>**

---

This is an author produced version of a paper published in **Biomaterials**.

White Rose Research Online URL for this paper:  
<http://eprints.whiterose.ac.uk/5234/>

---

**Published paper**

Korossis, S., Bolland, F., Southgate, J., Ingham, E. and Fisher, J. (2009)  
*Regional biomechanical and histological characterisation of the passive porcine urinary bladder: Implications for augmentation and tissue engineering strategies.*  
Biomaterials, 30 (2). pp. 266-275.

---

**Regional Biomechanical and Histological Characterisation of the  
Passive Porcine Urinary Bladder: Implications for Augmentation  
and Tissue Engineering Strategies**

**Sotirios Korossis, PhD** (*Corresponding Author*)

Institute of Medical and Biological Engineering

University of Leeds, Leeds, LS2 9JT, United Kingdom

E-mail: [s.korossis@leeds.ac.uk](mailto:s.korossis@leeds.ac.uk)

Tel. no: 0113 343 2197

Fax no: 0113 242 4611

**Fiona Bolland, PhD**

Jack Birch Unit of Molecular Carcinogenesis, Department of Biology, University of  
York, Heslington, York, YO10 5YW, United Kingdom.

**Jenny Southgate, PhD**

Jack Birch Unit of Molecular Carcinogenesis, Department of Biology, University of  
York, Heslington, York, YO10 5YW, United Kingdom.

**Eileen Ingham, PhD**

Institute of Medical and Biological Engineering, University of Leeds, Leeds, LS2 9JT,  
United Kingdom.

**John Fisher, PhD, DEng**

Institute of Medical and Biological Engineering, University of Leeds, Leeds, LS2 9JT,  
United Kingdom.

## Abstract

The aim of this study was to identify and quantify potential regional and directional variations in the quasistatic uniaxial mechanical properties of the passive urinary bladder wall. Overall, the lower body and trigone regions demonstrated the highest degree of directional anisotropy, whereas the ventral region demonstrated the least directional anisotropy. Significant regional anisotropy was found only along the apex-to-base direction. The dorsal and ventral regions demonstrated a significantly increased distensibility along the apex-to-base direction compared to the other bladder regions, whereas the trigone and lower body regions demonstrated the least distensibility. The trigone, lower body and lateral regions also demonstrated the highest tensile strength both at regional and directional level. The study detected significant regional and directional anisotropy in the mechanical properties of the bladder and correlated this anisotropy to the distended and non-distended tissue histioarchitecture and whole organ mechanics. By elucidating the inhomogeneous nature of the bladder, the results from this study will aid the regional differentiation of bladder treatments in terms of partial bladder replacement with suitable natural or synthetic biomaterials, as well as the development of more realistic constitutive models of bladder wall biomechanics and improved computational simulations to predict deformations in the natural and augmented bladder.

## Introduction

A variety of congenital and acquired conditions result in bladder dysfunction with consequent debilitating incontinence, which affects approximately 400 million people worldwide. In the majority of cases, a decrease in compliance is caused by thickening of the bladder wall due to smooth muscle cell hypertrophy and increased connective tissue deposition [1]. This may arise due to increased distension of the bladder wall (e.g. due to bladder outlet obstruction), which may directly or indirectly act as a stimulus for hypertrophy and hyperplasia [2,3,4,5]. Furthermore, neuropathic disease or trauma can induce significant alterations in the neural control of the bladder, which in turn can cause substantial changes in bladder function. These functional changes can produce severe alterations in the structure, thickness, compliance and biomechanics of the bladder wall [6,7,8]. Currently, the major surgical solution to restore lost function due to trauma, neurogenic or vascular dysfunction, or cancer is bladder augmentation surgery. Bowel is most commonly used in various procedures of neobladder replacement, such as augmentation enterocystoplasty or substitution enterocystoplasty. However, its use is not without long-term complications [9,10,11], suggesting that the materials used for the repair may be inadequate. In fact, rupture of the repaired bladder wall is known to occur in ~5% of cases [12]. The lack of an entirely satisfactory clinical procedure has led researchers to pursue alternative bladder replacement materials involving tissue engineering techniques [13,14].

Ideal materials for complete or partial bladder replacement should possess both biological compatibility, to promote cellular and tissue integration, and mechanical reliability. In order to design more appropriate long-term surgical repair procedures and develop materials for bladder reconstruction, and indeed to gain an insight into

1  
2  
3  
4 the disease processes that lead to bladder dysfunction, it is necessary to  
5  
6 characterize and quantify the fundamental mechanical properties of the normal  
7  
8 bladder at the mesoscale-tissue level and correlate them to both whole organ  
9  
10 mechanics and tissue histioarchitecture. Quantitative linking of the mechanics to  
11  
12 bladder histioarchitecture will also help to elucidate the repercussion of cellular and  
13  
14 molecular level alterations on bladder function [15]. Along these lines, studies have  
15  
16 correlated alterations in myosin isoform and collagen type content to force  
17  
18 development in bladder muscle strips [16,17] or to urodynamics data [18,19]. Such  
19  
20 correlations are important not only for interpreting structural/functional changes in  
21  
22 studying patterns of bladder dysfunction, but also to predict the fate of replacement  
23  
24 materials when exposed to the local normal or pathological mechanical loading in the  
25  
26 bladder wall *in vivo*.  
27  
28  
29

30  
31 In addition to the active contraction of the detrusor smooth muscle, the bladder  
32  
33 demonstrates nonlinear elastic, viscous and plastic mechanical properties  
34  
35 [20,21,22,23,24,25,26], depending on the boundary conditions. However, during  
36  
37 normal physiological filling rates bladder deformation can be considered quasistatic  
38  
39 [27], whereas neural and contractile effects are minimal [28]. Over the years, several  
40  
41 mathematical models have been developed in an effort to predict the stress-strain  
42  
43 behaviour of the bladder wall. Most of these models assume isotropy, homogeneity,  
44  
45 incompressibility and a spherical shape for the bladder wall [22,29,30,31]. Although  
46  
47 the assumptions of a spherical shape and incompressibility can give a relatively good  
48  
49 description of bladder mechanics during filling [32], it is questionable how descriptive  
50  
51 are the assumptions of isotropy and homogeneity for the bladder wall. The bladder  
52  
53 demonstrates a considerable inherent inhomogeneity in its material properties [33],  
54  
55 and as a result, it does not stretch equally in all directions, demonstrating areas of  
56  
57  
58  
59  
60  
61  
62  
63  
64  
65

1  
2  
3  
4 higher stretching and, subsequently, higher stress. In spite of this, relatively little is  
5  
6 known about the anisotropic mechanical properties of the bladder wall in terms of  
7  
8 direction or region, and only a meagre few studies have focused on this issue  
9  
10 [34,35]. As a first step towards the development of tissue engineered bladder repair  
11  
12 materials, the authors performed the first regional and directional mechanical  
13  
14 characterisation of the urinary bladder. In particular, the objective of this study was to  
15  
16 identify and quantify potential regional and directional variations in the passive  
17  
18 mechanical properties of the bladder wall and correlate these variations to its  
19  
20 histioarchitecture and whole organ mechanics. By elucidating the inhomogeneous  
21  
22 nature of the bladder, the aim of this work was to consider the implications for  
23  
24 developing suitable natural or synthetic biomaterials for bladder augmentation.  
25  
26  
27  
28

## 29 30 **Materials & Methods**

### 31 32 *Specimen procurement & dissection*

33  
34 Intact bladders from 16-week-old commercial male pigs were collected from a  
35  
36 local abattoir and transported to the laboratory on ice in transport medium [Hanks'  
37  
38 balanced salt solution without  $\text{Ca}^{++}$  and  $\text{Mg}^{++}$  (HBSS, Invitrogen, Paisley, UK)  
39  
40 containing 10 mM HEPES, pH 7.6 (Invitrogen) and 10 KIU/ml Aprotinin (Trasylol,  
41  
42 Bayer, Berkshire, UK)] [36]. The absence of calcium in the solution helped ensure  
43  
44 that the bladders were in an inactivated state and that no spontaneous contractions  
45  
46 would occur during testing. Prior to testing, the bladders were sized by photographing  
47  
48 them in their deflated/non-distended state (Figure 1). The recorded images of the  
49  
50 bladders were calibrated and the maximum bladder width along the circumferential  
51  
52 direction was measured using an image analysis software (Image Pro Plus<sup>TM</sup>,  
53  
54 MediaCybernetics®). The average size of the bladders used in this study was  $68 \pm$   
55  
56  $11.7$  mm (mean  $\pm$  95% confidence interval,  $n = 6$ ).  
57  
58  
59  
60  
61  
62  
63  
64  
65

The bladders were subsequently dissected along the apex-to-base line, as show in Figure 2a, and samples were isolated from the dorsal, trigone, lateral, ventral and lower body regions of the wall, as well as along the apex-to-base (longitudinal) and transverse (circumferential) directions (Figure 2b). For the purpose of the biomechanical characterization, specimens measuring 20×5 mm were isolated using a purpose-built block cutter [37]. From each bladder, one apex-to-base and one transverse specimen were isolated from each one of the five anatomical regions. Samples from the five anatomical regions and along the two directions were also harvested for histological examination. Following isolation, the specimens were stored in transport medium and tested either biomechanically or histologically within 6 hours from slaughter.

#### *Histological characterisation*

Histological examination was performed on samples harvested along the apex-to-base and transverse directions from the five anatomical regions of the bladder wall, in order to analyse the general histioarchitecture, as well as the amount and orientation of elastin, collagen and smooth muscle. The samples were retrieved either from the procured empty bladders and fixed in 10% (v/v) neutral buffered formalin (NBF), or from a bladder that had been distended to the mean physiological capacity with 500 ml of 10% (v/v) NBF. Post-fixation, distended and non-distended samples were dehydrated and embedded in paraffin wax. Histological sections were stained with either Miller's stain to evaluate the content and distribution of elastin, Van Gieson's stain to evaluate the distribution of collagen and smooth muscle, or with haematoxylin and eosin (H&E) [38]. The stained sections were examined under light microscopy and photographed.

#### *Biomechanical characterisation*



Bladder wall strips were subjected to low-strain rate uniaxial tensile loading to failure in order to investigate potential regional variations in the passive stress strain-behaviour of the bladder wall. In addition, the directional anisotropy of the bladder wall was investigated by testing specimens along the apex-to-base and transverse directions. In total, 10 test groups of 6 specimens each were studied. Prior to testing, the thickness of the samples was measured at 6 points along their long axis using a gauge with a resolution of 0.01 mm (Mitutoyo, Andover, UK), and their average thickness ( $t$ ) was recorded. Subsequently, the samples were mounted onto a purpose-built titanium holder. The holder was supported by a removable aluminium bracket that allowed alignment of the two holder grips, defined the gauge length of the specimens, and ensured that no load was imposed on the specimen until the start of the test [37]. The gauge length of the specimens was defined by a 10 mm wide central block separating the two holder parts and screwed onto the bracket. Once a sample was clamped onto the holder, the holder with the supporting bracket was secured to a Howden tensile machine and the bracket was removed. Prior to loading to failure, the specimens were preconditioned under cyclic loading using a double-ramp wave function at a rate of 10 mm/min. A preconditioning regime of 10 cycles was sufficient to produce a steady-state load-elongation response from the samples. Following preconditioning, the samples were sequentially stretched to failure at a rate of 10 mm/min. All testing was conducted in physiologic saline (0.9% w/v NaCl) and at room temperature. Total testing time was approximately 3 min per specimen. During testing, load data from the load cell and specimen extension data from the stroke of the cross-head of the tensile testing machine was acquired at a rate of 20Hz.

1  
2  
3  
4 In order to obtain an accurate measure of the tissue gauge length, the tensile  
5  
6 machine was set to produce a specimen preloading of 0.02 N before the operating  
7  
8 program started to acquire any data. Therefore, zero extension was taken at the  
9  
10 point where a load of 0.02 N was detected. The final gauge length ( $L_o$ ) of the  
11  
12 specimen was calculated as the initial gauge length (10 mm) plus the extension that  
13  
14 was needed to produce the specified preloading. Failure was taken to occur when  
15  
16 the first decrease in load was detected during extension. The mode of failure  
17  
18 observed was middle section necking and rupture for all of the specimens tested.  
19  
20 The recorded load ( $F$ ) and specimen extension data ( $\Delta L$ ) from the loading to failure  
21  
22 phase of each specimen was converted to stress and strain. Stress ( $\sigma$ ) was defined  
23  
24 in the Lagrangian sense as  $F/\text{unloaded cross-sectional area}$ , whereas the  
25  
26 percentage in-plane axial strain ( $\varepsilon$ ) was defined as  $(\Delta L/L_o) \times 100\%$  [39]. The calculated  
27  
28 stress-strain responses obtained for the specimens of each group were averaged  
29  
30 over the number of specimens in each group ( $n = 6$ ) using a mathematical analysis  
31  
32 software package (Origin v6.0, Microbal). Moreover, the stress-strain behaviour of  
33  
34 each specimen was analyzed by means of six parameters. These have been  
35  
36 described elsewhere [37] and included the elastin (EI-E) and collagen (Col-E) phase  
37  
38 slopes, transition stress ( $\sigma_{\text{trans}}$ ) and strain ( $\varepsilon_{\text{trans}}$ ), ultimate tensile strength ( $\sigma_{\text{uts}}$ ) and  
39  
40 failure strain ( $\varepsilon_{\text{uts}}$ ). The biomechanical parameters were analyzed by one-way  
41  
42 analysis of variance (ANOVA) and the individual means from each group were  
43  
44 compared using the Student's t-test to calculate the minimum significant difference at  
45  
46 the 95% and 99% confidence levels.  
47  
48  
49  
50  
51  
52  
53  
54

55 In an attempt to link the passive mesoscale-tissue mechanical properties of the  
56  
57 bladder wall obtained from the uniaxial tensile tests with the mechanics of the whole  
58  
59 bladder, the calculated stress-strain data was converted to bladder intraluminal  
60  
61  
62  
63  
64  
65

pressure-bladder volume relationships using the law of Laplace for a thin-walled sphere. While no complete survey of bladder shapes was performed, the reports of the shapes of normal bladders tend to describe spherical bladders [40] and prolate spheroidal bladders [33]. Although these models are only rough approximations of the real bladder shape, it was deemed sufficient to use the spherical bladder assumption, together with the assumptions of homogeneity and isotropy entailed by the law of Laplace, to generate a qualitative correlation between mesoscale-tissue and organ scale properties. The purpose of this analysis was to examine how the whole bladder mechanics change if the regional and directional anisotropy inherent in the bladder wall is not taken into consideration.

The law of Laplace for a segment of homogeneous thin-walled sphere relates the internal pressure (P) applied to the segment, to its thickness (t) and radius (R), and the membrane stress ( $\sigma$ ) in the segment, according to [41]:

$$P = \frac{2t\sigma}{R} \quad (1)$$

Assuming an un-pressurised bladder arc segment of angle  $\theta$  and radius  $R_o$ , its original undeformed length is  $L_o = R_o \cdot \theta$ . When the segment is pressurised by an internal pressure P, its radius increases to R. In addition, its length increases by  $\Delta L$ , generating an axial membrane stress ( $\sigma$ ) along its length. The length of the pressurised segment is  $L = L_o + \Delta L = R \cdot \theta$ . Consequently, the radius R of the pressurised segment can be estimated by:

$$\frac{R}{R_o} = \frac{L_o + \Delta L}{L_o} = 1 + \varepsilon \quad (2)$$

$L_o$  represents the un-stretched gauge length of the tissue specimens (final gauge length, allowing for the preloading of 0.02 N) used in the uniaxial tensile tests,

whereas the ratio  $\Delta L/L_0$  is the in-plane axial strain ( $\varepsilon$ ) in the segment and represents the strain calculated from the uniaxial tensile tests for the tissue strips. Therefore, the internal bladder pressure was calculated according to:

$$P = \frac{2t\sigma}{R_0(1+\varepsilon)} \quad (3)$$

The membrane stress  $\sigma$ , produced by the stretch  $\Delta L$  in the bladder segment, represents the corresponding axial tensile stress calculated for the tissue strips under uniaxial tension. Moreover, the volume of the bladder, corresponding to the in-plane axial strain in the bladder segment, was estimated from the volume of the sphere and employing equation (2):

$$V = \frac{4}{3}\pi R_0^3(1+\varepsilon)^3 \Rightarrow V = V_0(1+\varepsilon)^3 \quad (4)$$

The internal diameter of the bladder was assumed to be 68 mm ( $R = 34$  mm), which was the averaged maximum width measured along the circumferential direction of the bladders used in the testing (Figure 1). Moreover, the bladder thickness was assumed to be the averaged group thickness of the bladder strips tested under uniaxial tension.

## Results

### *Histological characterisation*

The results of the structural analysis of the bladder wall, obtained from the histological staining of samples from the dorsal, ventral, lateral lower body, and trigone regions, as well as along the apex-to-base and transverse directions, are illustrated in Figure 3 for the non-distended bladders, and Figure 4 and Figure 5 for the bladder fixed while distended to 500 ml. Examination of the regional bladder histioarchitecture revealed that elastin was generally sparse in the bladder wall.

Nevertheless, among the five regions investigated, the samples retrieved from the dorsal, ventral and lateral regions contained the most elastin, whereas the samples from the lower body region contained the least amount of elastin (Figure 3). In all regions, elastin appeared to be oriented predominantly in the transverse (circumferential) direction (Figure 5). In the ventral region, elastin seemed to be concentrated in the lower half/serosa region, whereas the trigone region appeared to contain a scattering of elastin bundles. The detrusor muscle was most compact within the trigone region (Figure 3), but it was difficult to distinguish any discernible patterns of orientation that would discriminate one region from another. Samples retrieved from the lower body and trigone regions of the distended bladder were structurally the least affected by distension, retaining thickness and a convoluted urothelium (Figure 4). Upon distension, the dorsal, lateral and ventral regions reduced in thickness and the local urothelium was flattened. Miller's elastin staining showed the presence of elastin in vessel walls (Figure 5). Van Gieson's staining showed that the muscle bundles in the dorsal, lateral and ventral regions of the distended bladder were more compacted than in the trigone and lower body regions, reflecting the increased distension of these regions and the subsequent reorganisation of the ECM. This supports the observations in the non-distended bladder that the dorsal, ventral and lateral regions contained the most elastin and the lower body region the least. Elastin provides the recoiling mechanism in the tissues and it is usually present in regions of tissues which are subjected to increased deformations. Van Gieson's staining also revealed that the lateral, lower body and trigone regions expressed an increased network of collagen compared to the dorsal and ventral regions (Figure 5).

### *Biomechanical characterisation*

During uniaxial tensile loading to failure, the site of specimen failure was within the central region of the specimens, whereas there was no evidence of specimen slippage within the grips of the holder. The acquired force and elongation data for each specimen tested was converted to stress and strain, respectively, and the averaged apex-to-base and transverse stress-strain behaviours for each of the five regional groups were plotted on the same chart in order to examine the potential directional anisotropy of the bladder wall. These results are illustrated in Figure 6. The average biomechanical parameters obtained from the stress-strain behaviours of the specimens in each of the test groups are gathered in Figure 7. All groups demonstrated the typical quasistatic stress-strain behaviour of soft tissues comprising an initial linear region (elastin phase) followed by a secondary prolonged linear region (collagen phase) before failure. Comparatively to other soft tissues [37], the elastin phase of all groups was much shorter than the extent of the collagen phase, depicting the reduced amount of elastin in the bladder wall, relatively to its content in other ECM structures, observed under histological examination.

Overall, the specimens retrieved along the transverse direction from all regions, appeared to be more compliant, suggesting increased levels of deformation for the same levels of applied stress (Figure 6). However, significant directional anisotropy was present only in the stress-strain behaviour of the lateral, lower body, and trigone regions. Specifically, the lateral region showed significantly increased collagen phase slope ( $p = 0.027$ ) and ultimate tensile strength ( $p = 0.013$ ) along the apex-to-base direction (Figure 7). Statistically significant increase along the apex-to-base direction were also observed in the collagen phase slope ( $p = 0.003$ ), transition stress ( $p = 0.027$ ) and ultimate tensile strength ( $p = 0.036$ ) of the lower body region. The trigone

1  
2  
3  
4 region presented a significant increase in the collagen phase slope ( $p = 0.004$ ) and  
5  
6 significant decrease in the transition ( $p = 0.026$ ) and failure ( $p = 0.021$ ) strains in the  
7  
8 apex-to-base direction. In contrast, the dorsal region demonstrated the least  
9  
10 directional anisotropy, being in fact, quite isotropic in the whole range of its stress-  
11  
12 strain behaviour ( $p > 0.05$ ). In between the two extremes, the ventral region also  
13  
14 demonstrated a degree of directional anisotropy, which was limited to a decrease in  
15  
16 the transition strain ( $p = 0.013$ ) of the apex-to-base direction.  
17  
18

19  
20 In order to produce a quantitative comparison of the degree of directional  
21  
22 anisotropy between the five anatomical regions, the ratio of the collagen phase  
23  
24 slopes between the apex-to-base and transverse direction groups of each of the five  
25  
26 regions was calculated and presented in Table 1. These ratios indicated that the  
27  
28 lower body region expressed the highest degree of anisotropic behaviour, with a  
29  
30 collagen phase slope along the apex-to-base direction more than 3 times bigger than  
31  
32 the one along the transverse direction. The smallest ratios were calculated for the  
33  
34 dorsal and ventral regions, which demonstrated similar collagen phase slopes along  
35  
36 their apex-to-base and transverse directions.  
37  
38

39  
40 Analysis of the biomechanical parameters also revealed significant regional  
41  
42 anisotropy in the bladder wall. However, this anisotropy was confined only in the  
43  
44 apex-to-base direction between the five anatomical regions (Figure 7). Statistically  
45  
46 significant differences were found in all biomechanical parameters studied except for  
47  
48 the case of the elastin phase slope. In the extra-physiological stress range (collagen  
49  
50 phase) significant differences were observed in the collagen phase slopes of the  
51  
52 dorsal and ventral regions which were reduced compared to the trigone region ( $p =$   
53  
54  $0.020$ ), and the lateral ( $p = 0.043$ ), lower body ( $p = 0.006$ ) and trigone regions ( $p =$   
55  
56  $0.001$ ), respectively. This indicated a significantly increased compliance of the dorsal  
57  
58  
59  
60  
61  
62  
63  
64  
65

1  
2  
3  
4 and ventral compared to the other bladder regions. Moreover, the ultimate tensile  
5  
6 strength of the ventral region was significantly reduced compared to the lateral ( $p =$   
7  
8 0.028) and lower body ( $p = 0.046$ ) regions, whereas the transition stress of the lower  
9  
10 body was significantly increased compared to the dorsal region ( $p = 0.483$ ). With  
11  
12 regards to the extensibility of the bladder wall, the trigone region was the least  
13  
14 distensible, demonstrating significantly reduced transition and failure strains  
15  
16 compared to the dorsal ( $p = 0.005$  &  $0.004$ ), ventral ( $p = 0.017$  &  $0.012$ ), lateral ( $p =$   
17  
18  $0.001$  &  $0.002$ ), and lower body ( $p = 0.001$  &  $0.004$ ) regions. The combined findings  
19  
20 of this study with regards to the regional anisotropy of the bladder wall along the  
21  
22 apex-to-base direction are illustrated in Figure 8, which illustrates the variation of the  
23  
24 collagen phase slope, ultimate tensile strength, transition strain and failure strain  
25  
26 over the five anatomical regions investigated.  
27  
28  
29

30  
31 The mesoscale-tissue mechanical properties obtained from the uniaxial tensile  
32  
33 tests were correlated to whole bladder mechanics by converting the stress-strain  
34  
35 behaviour of each specimen in each of the ten test groups to a pressure-volume  
36  
37 response. The purpose was to predict pressure-volume relationships for the whole  
38  
39 organ, assuming a regionally and directionally isotropic, homogeneous and spherical  
40  
41 bladder. Subsequently, the converted pressure-volume results for each specimen  
42  
43 were averaged over the number of specimens in each group and plotted for the  
44  
45 physiological bladder volume interval, which was assumed to be  $\approx 500$  ml (Figure 9).  
46  
47  
48 In essence, these pressure-volume relationships represent the behaviour of the  
49  
50 whole bladder assuming that its mechanical properties are uniform and identical to  
51  
52 the properties of each of the individual test groups. Analysis of these results indicated  
53  
54 that there were significant differences in the slopes of the pressure-volume profiles  
55  
56 calculated individually for each specimen and averaged for the specimens in each  
57  
58  
59  
60  
61  
62  
63  
64  
65



group (Figure 10). The slope of the model employing the properties of the trigone region along the apex-to-base direction was significantly increased compared to the dorsal (apex-to-base,  $p = 0.046$ ), ventral (transverse,  $p = 0.047$ ), lower body (apex-to-base, transverse;  $p = 0.034$  &  $0.016$ , respectively), and trigone (transverse,  $p = 0.047$ ) models.

## Discussion

The aim of this study was to investigate the homogeneity and anisotropy of the passive urinary bladder with regards to the mechanical properties and histioarchitecture of the bladder wall. This was the first study, to the knowledge of the authors, which used uniaxial mechanical testing to investigate the regional and directional anisotropy of the urinary bladder, and to correlate the mesoscale-tissue mechanical properties to the whole organ pressure-volume behaviour. Over the years, the quasistatic mechanical properties of the bladder have been characterised utilising tensile loading tests [34,35,42,43,44] and *in vivo* studies [44,45,46,47]. *In vivo* whole organ testing cannot directly determine bladder wall tissue properties due to regional differences, and can be affected by neural influences and intrinsic muscle activity, as well as other concomitant variables such as non-uniform wall stress distribution and external loading by the pelvic organs [35]. Tensile loading tests on bladder wall samples have focused on uniaxial [32,42,43] or biaxial [34,35] protocols. Admittedly, biaxial mechanical testing produces a more physiological loading state as the bladder wall is loaded in all three dimensions *in vivo*. In addition, phenomena such as mechanical cross-coupling, describing how the stress level in one direction can affect the stress-strain behaviour in the other, which can be important in studying biaxial tissues, can be better appreciated under biaxial testing. An improvement to the existing testing methodology would be to employ biaxial testing alongside the

1  
2  
3  
4 uniaxial protocol. Nevertheless, uniaxial testing is an attractive investigation tool  
5  
6 because it localises the investigation to a very small area of the organ from which a  
7  
8 tissue sample can be isolated and subjected to controlled stress states. This is a  
9  
10 particularly well suited approach when investigating anisotropic behaviour of tissues.  
11  
12 Since the purpose of this study was not to fully characterise the mechanical  
13  
14 properties of the bladder in terms of a constitutive three-dimensional model, in which  
15  
16 case a biaxial testing protocol would be more appropriate, but to investigate its  
17  
18 potential anisotropy and inhomogeneity, it was deemed appropriate to use uniaxial  
19  
20 tensile testing.  
21  
22

23  
24         The regional and directional anisotropy of the bladder has attracted surprisingly  
25  
26 little attention over the years. A meagre few studies have focused on the anisotropy  
27  
28 of the mechanical properties of the bladder [34,35], and even these have  
29  
30 concentrated on the directional anisotropy. In addition to the directional anisotropy,  
31  
32 this study also identified a regional anisotropy inherent in the mechanical properties  
33  
34 of the bladder wall. Moreover, the magnitudes of the biomechanical parameters  
35  
36 calculated in this study were comparable to those reported by others for porcine  
37  
38 bladder tissue [42], considering the differences in experimental protocols, as well as  
39  
40 in the methods used to estimate tissue thickness which have a direct impact on the  
41  
42 magnitude of the estimated stress. With regards to the directional anisotropy, the  
43  
44 specimens retrieved along the transverse direction from all regions appeared to be  
45  
46 more compliant (increased transition and failure strains, reduced collagen phase  
47  
48 slopes) compared to the apex-to-base specimens. The increased compliance along  
49  
50 the transverse direction, which was more profound in the extra-physiological  
51  
52 mechanical properties, indicated that at the organ level the bladder distends more in  
53  
54 this direction than along the apex-to-base one. Within the physiological distension  
55  
56  
57  
58  
59  
60  
61  
62  
63  
64  
65

limits (up to approximately the transition point of the stress-strain curve), the increased compliance observed along the transverse direction was supported by the histological results, which indicated that elastin was predominantly oriented in the transverse direction (Figure 5). Elaborating, elastin provides the recoiling mechanism in the tissues and it is most abundant in tissues, or regions of tissues, subject to increased stretching during physiological function [48]. Directional anisotropy was also observed in the ultimate tensile strength of the specimens, with the specimens retrieved along the transverse direction from all regions achieving lower strengths than the apex-to-base specimens. The difference, though, was significant only in the lateral and lower body regions. Overall, the lower body demonstrated the highest degree of directional anisotropy, whereas the dorsal and ventral region demonstrated the least directional anisotropy (Figure 6 & Table1).

Significant regional anisotropy in the bladder wall was found only along the apex-to-base direction (Figure 7 & 8). The lack of any significant regional anisotropy along the transverse direction indicates that the organ experiences a rather uniform circumferential expansion. Statistically significant differences were found in all biomechanical parameters except in the slope of the elastin phase. The dorsal and ventral regions demonstrated a significantly increased compliance along the longitudinal direction compared to the other bladder regions, as indicated by the reduced collagen phase slope and transition stress, and increased transition and failure strain of these regions. The reduced transition stress of these regions indicates that they can reach their transition point, at which the collagen and smooth muscle fibres have uncrimped and begin to bear all the applied load, with less effort (less pressure) than the other regions. As a complementary effect, the significantly increased transition strain of the dorsal and ventral regions, as well as of the lateral

1  
2  
3  
4 region, compared to the trigone, indicates that with the same effort (same pressure)  
5  
6 these regions are prone to deform more than the trigone in the apex-to-base  
7  
8 direction. In fact, the trigone region demonstrated the least distensibility, experiencing  
9  
10 the lowest transition and failure strains and the highest collagen phase slope in both  
11  
12 directions (although not significantly so in the transverse) compared to the other  
13  
14 regions (Figure 7 & 8). The second highest collagen phase slope and lowest failure  
15  
16 strain was demonstrated by the lower body region. The findings of the increased  
17  
18 compliance of the dorsal, ventral and lateral regions compared to the trigone and  
19  
20 lower body regions were supported by the increased elastin network found in these  
21  
22 regions, as well as by the fact that histological samples retrieved from the lower body  
23  
24 and trigone regions of the distended bladder were structurally the least affected by  
25  
26 distension. The trigone, lower body and lateral regions also demonstrated the highest  
27  
28 tensile strength both at regional and directional level. This can be attributed to the  
29  
30 increased networks of collagen, the main function of which in connective tissues is to  
31  
32 withstand tension, as well as to the thicker layers of muscle, observed in these  
33  
34 regions under histological examination.  
35  
36  
37  
38  
39

40       The directional and regional anisotropy in the mesoscale-tissue mechanical  
41  
42 properties of the bladder was inherited in the whole organ mechanics when the  
43  
44 stress-strain behaviours of the different regions were used to model pressure-volume  
45  
46 relationships for the whole organ. The purpose was to investigate whether  
47  
48 mesoscale-tissue mechanical properties can be translated to meaningful whole organ  
49  
50 mechanics, given an appropriate model for the bladder shape and how the wall  
51  
52 stretch is distributed in the bladder wall. The assumptions of a spherical geometry,  
53  
54 homogeneity and anisotropy do not constitute a realistic bladder model.  
55  
56  
57  
58 Nevertheless, this model was sufficient to examine how the whole pressure-volume  
59  
60  
61  
62  
63  
64  
65

relationship of bladder changes if the mechanical properties of a particular bladder region are adopted as universal bladder properties. Although these results were at best estimates based on assumptions of homogeneity, and only descriptive of whole bladder mechanics, they were indicative of the inherent regional and directional anisotropy present in the bladder. The modelled pressure-volume profiles were in general agreement with similar data obtained from bladder cystometry [49]. However, there was a considerable scatter among the results of the individual regions and directions. The scatter ranged from a model describing a bladder that offers considerable resistance to deformation, by employing the results of the trigone region along the apex-to-base direction, to a bladder that is quite compliant and offers little resistance to deformation, by employing the results of the ventral region along the transverse direction. Moreover, the pressure-volume models verified the lack of any significant anisotropy along the transverse direction of the anatomical regions, with the models assuming the properties of the transverse regional groups clustering together, towards the compliant bladder region.

## Conclusions

This study detected significant regional and directional anisotropy in the quasistatic uniaxial mechanical properties of the passive urinary bladder and correlated this anisotropy to the distended and non-distended tissue histioarchitecture and whole organ mechanics. The experimental protocol used to evaluate the mesoscale mechanical properties of the bladder by employing uniaxial tensile testing was effective in detecting bladder anisotropy. Differences between isotropic and anisotropic behaviour can become important in regions of high stress and in bladder augmentation surgery that changes the natural shape and boundary conditions of the bladder. In general, the results from this study will aid the regional

1  
2  
3  
4 differentiation of bladder treatments in terms of partial bladder replacement, as well  
5  
6 as the development of more realistic constitutive models of bladder wall  
7  
8 biomechanics and improved computational simulations to predict deformations in the  
9  
10 natural and augmented bladder.  
11  
12  
13

## 14 **Acknowledgements**

15  
16 This work was funded by the Biotechnology and Biological Sciences Research  
17  
18 Council (BBSRC Grant E20352). SK is funded by the Engineering and Physical  
19  
20 Sciences Research Council.  
21  
22  
23  
24  
25  
26  
27  
28  
29  
30  
31  
32  
33  
34  
35  
36  
37  
38  
39  
40  
41  
42  
43  
44  
45  
46  
47  
48  
49  
50  
51  
52  
53  
54  
55  
56  
57  
58  
59  
60  
61  
62  
63  
64  
65

## References

1. Chang SL, Chung JS, Yeung MK, Howard PS, Macarak EJ. Roles of the lamina propria and the detrusor in tension transfer during bladder filling. *Scand J Urol Nephrol Suppl* 1999; 201:38-45.
2. Elbadawi A, Meyer S, Regnier CH. Role of ischemia in structural changes in the rabbit detrusor following partial bladder outlet obstruction: a working hypothesis and a biochemical/structural model proposal. *Neurourol Urodynam* 1989; 8: 151-162.
3. Gabella G. Hypertrophy of visceral smooth muscle. *Anat Embryol* 1990; 182:409-424.
4. Kitada S, Wein AJ, Kato K, Levin RM. Effect of acute complete obstruction on the rabbit urinary bladder. *J Urol* 1989; 141: 166-169.
5. Tammela TLJ, Levin RM, Monson FC, Wein AJ, Longhurst PA. The influence of acute over-distension on rat bladder function and DNA synthesis. *J Urol* 1993; 150:1533-1539.
6. German K, Bedwani J, Davies J, Brading AF, Stephenson TP. An assessment of the contribution of visco-elastic factors in the aetiology of poor compliance in the human neuropathic bladder. *Br J Urol* 1994; 74(6):744-748.
7. Watanabe T, Rivas DA, Chancellor MB. Urodynamics of spinal cord injury. *Urol Clin North Am* 1996; 23(3):459-473.
8. Kruse MN, Bray LA, de Groat WC. Influence of spinal cord injury on the morphology of bladder afferent and efferent neurons. *J Auton Nerv Syst* 1995; 54(3):215-224.

9. Bunyaratavey P, Lao S, Kongkanand A, Brasopsanti K, Vajrapongse R. Ten years' experience with enterocystoplasty. *J Med Assoc Thai* 1993; 76: 327–333.
10. Khoury JM, Timmons SL, Corbel L, Webster GD. Complications of enterocystoplasty. *Urology* 1992; 40: 9–14.
11. Greenwell TJ, Venn SN, Mundy AR. Augmentation cystoplasty. *BJU Int.* 2001; 88(6):511-25.
12. Chancellor MB, Rivas DA, Bourgeois IM. Laplace's law and the risks and prevention of bladder rupture after enterocystoplasty and bladder autoaugmentation. *Neurourol Urodyn* 1996;15(3):223-233.
13. Bolland F, Korossis S, Wilshaw SP, Ingham E, Fisher J, Kearney JN *et al.* Development and characterisation of a full-thickness acellular porcine bladder matrix for tissue engineering. *Biomaterials* 2007 Feb; 28(6):1061-1070.
14. Southgate J, Cross W, Eardley I, Thomas DF, Trejdosiewicz LK. Bladder reconstruction-from cells to materials. *Proc Inst Mech Eng [H]*. 2003; 217(4):311-316.
15. Korossis S, Bolland F, Ingham E, Fisher J, Kearney J, Southgate J. Review: tissue engineering of the urinary bladder: considering structure-function relationships and the role of mechanotransduction. *Tissue Eng* 2006; 12(4):635-644.
16. Roelofs M, Wein AJ, Monson FC, Passeriniglazel G, Koteliansky VE, Sartore S *et al.* Contractility and phenotype transitions in serosal thickening of obstructed rabbit bladder. *J Appl Physiol* 1995; 78: 1432–41.
17. Wang Z, Gopalakurup SK, Levin RM, Chacko S. Expression of smooth muscle myosin isoforms in urinary bladder smooth muscle during hypertrophy and regression. *Lab Invest* 1995; 73: 244–51.



18. Baskin LS, Constantinescu S, Duckett JW, Snyder HM, Macarak E. Type III collagen decreases in normal foetal bovine bladder development. J Urol 1994; 152: 688–91.
19. Landau EH, Jayanthi VR, Churchill BM, Shapiro E, Gilmour RF, Khoury AE *et al*. Loss of elasticity in dysfunctional bladders: urodynamic and histochemical correlation. J Urol 1994; 152: 702–5.
20. Venegas JG. Viscoelastic properties of the contracting detrusor: I. theoretical basis. Am J Physiol 1991; 261:C355–363.
21. Finkbeiner AE, O'Donnell PD. Responses of detrusor smooth muscle to stretch and relaxation: in vitro study. Urology 1990; 36: 193–198.
22. Regnier CH, Kolsky H, Richardson PD, Ghoniem GM, Susset JG. The elastic behavior of the urinary bladder for large deformations. J Biomech 1983; 16: 915–922.
23. Coolsaet BL, van Mastrigt R, Van Duyl WA, Huygen RE. Viscoelastic properties of bladder wall strips at constant elongation. Invest Urol 1976; 13: 435–440.
24. Coolsaet BL, van Duyl WA, van Mastrigt R, van der Zwart A. Visco-elastic properties of the bladder wall. Urol Int 1975; 30: 16–26.
25. Alexander RS. Viscoplasticity of smooth muscle of urinary bladder. Am J Physiol 1973; 224: 618–622.
26. Kondo A, Susset JG. Physical properties of the urinary detrusor muscle. A mechanical model based upon the analysis of stress relaxation curve. J Biomech 1973; 6: 141–151.

- 1  
2  
3  
4 27. Klevmark B. Motility of the urinary bladder in cats during filling at physiological  
5 rates. I. Intravesical pressure patterns studied by a new method of cystometry. *Acta*  
6  
7  
8 *Physiol Scand* 1974; 90: 565–577.  
9
- 10  
11 28. Klevmark B. Motility of the urinary bladder in cats during filling at physiological  
12 rates. II. Effects of extrinsic bladder denervation on intramural tension and on  
13 intravesical pressure patterns. *Acta Physiol Scand* 1977; 101: 176–184.  
14  
15  
16  
17  
18 29. Tözeren A. Assessment of fiber strength in a urinary bladder by using  
19 experimental pressure volume curves: an analytical method. *J Biomech Eng* 1986;  
20 108:301-305.  
21  
22  
23  
24  
25 30. Van Mastrigt R, Griffiths DJ. An evaluation of contractility parameters  
26 determined from isometric contractions and micturition studies. *Urol Res* 1986; 14:45-  
27 52.  
28  
29  
30  
31  
32 31. Damaser MS, Lehman SL. The effect of urinary bladder shape on its mechanics  
33 during filling. *J Biomechanics* 1995; 28(6):725-732.  
34  
35  
36  
37  
38 32. Andersson KE, Arner A. Urinary bladder contraction and relaxation: physiology  
39 and pathophysiology. *Physiol Re* 2004; 84:935-986.  
40  
41  
42  
43 33. Gabella G, Uvelius B. Urinary bladder of rat: fine structure of normal and  
44 hypertrophic musculature. *Cell Tissue Res* 1990; 262:67–79.  
45  
46  
47  
48 34. Gloeckner D, Sacks M, Chancellor M, de Groat W. Active and passive biaxial  
49 mechanical properties of urinary bladder wall. In: *Engineering in Medicine and*  
50 *Biology*. 21st Annual Conf. and the 1999 Annual Fall Meeting of the Biomedical  
51 Engineering Society BMES/EMBS Conference. 1999; 1:17.  
52  
53  
54  
55  
56  
57  
58  
59  
60  
61  
62  
63  
64  
65

- 1  
2  
3  
4 35. Gloeckner DC, Sacks MS, Fraser MO, Somogyi GT, de Groat WC, Chancellor  
5 MB. Passive biaxial mechanical properties of the rat bladder wall after spinal cord  
6 injury. J Urol. 2002; 167(5):2247-2252.  
7  
8  
9
- 10 36. Southgate J, Masters JR, Trejdosiewicz LK. Culture of human urothelium. In:  
11 Freshney RI FM, editor. Culture of epithelial cells. 2nd ed. New York: Wiley. 2002;  
12 381–400.  
13  
14  
15  
16  
17
- 18 37. Korossis S, Booth C, Wilcox HE, Watterson KG, Kearney JN, Ingham E *et al.*  
19 Tissue engineering of cardiac valve prostheses II: Biomechanical characterisation of  
20 decellularised porcine aortic heart valves. J Heart Valve Dis. 2002; 11(4):463-471.  
21  
22  
23  
24
- 25 38. Bancroft J, Stevens A. Theory and practice of histological techniques. London:  
26 Churchill Livingstone. 1990.  
27  
28  
29
- 30 39. Korossis S, Wilcox HE, Watterson KG, Kearney JN, Ingham E, Fisher J. In-vitro  
31 assessment of the functional performance of the decellularised intact porcine aortic  
32 root. J Heart Valve Dis. 2005; 14(3):408-422.  
33  
34  
35  
36  
37
- 38 40. Griffiths CJ, Assi MS, Styles RA, Ramsden PD, Neal DE. Ambulatory  
39 monitoring of bladder and detrusor pressure during natural filling. J Urol 1989;  
40 142:780–784.  
41  
42  
43  
44
- 45 41. Fung YCB. Biomechanics, mechanical properties of living tissues. 2nd ed,  
46 Springer-Verlag, New York 1993; 14-20.  
47  
48  
49
- 50 42. Dahms E, Piechota HJ, Dahiya R Lue TF, Tanagho EA. Composition and  
51 biomechanical properties of the bladder acellular matrix graft: comparative analysis in  
52 rat, pig and human. Br J Urol 1998; 82:411-419.  
53  
54  
55  
56
- 57 43. Alexander RS. Series elasticity of urinary bladder smooth muscle. Am J Physiol  
58 1976; 231:1337.  
59  
60  
61  
62  
63  
64  
65

- 1  
2  
3  
4 44. Alexander RS. Mechanical properties of urinary bladder. Am J Physiol 1971;  
5  
6 220:1413.  
7  
8  
9 45. Rohrmann D, Zderic SA, Duckett JW, Levin RM, Damaser MS. Compliance of  
10 the obstructed foetal rabbit bladder. Neurourol Urodyn 1997; 16(3):179-189.  
11  
12  
13 46. Coplen DE, Macarak EJ, Levin RM. Developmental changes in normal foetal  
14 bovine whole bladder physiology. J Urol 1994; 151:1391.  
15  
16  
17  
18 47. Levin RM, Horan P, Liu SP. Metabolic aspects of urinary bladder filling. Scand J  
19 Urol Nephrol suppl. 1999; 201:59.  
20  
21  
22  
23 48. Viidik A, Danielsen CC, Oxlund H. On fundamental and phenomenological  
24 models, structure and mechanical properties of collagen and elastin and  
25 glycosaminoglycan complexes. Biorheology 1982; 19: 437–451.  
26  
27  
28  
29 49. Damaser MS. Whole bladder mechanics during filling. Scand J Urol Nephrol  
30 Suppl 1999; 201:51–58  
31  
32  
33  
34  
35  
36  
37  
38  
39  
40  
41  
42  
43  
44  
45  
46  
47  
48  
49  
50  
51  
52  
53  
54  
55  
56  
57  
58  
59  
60  
61  
62  
63  
64  
65

Figure 1

Figure1

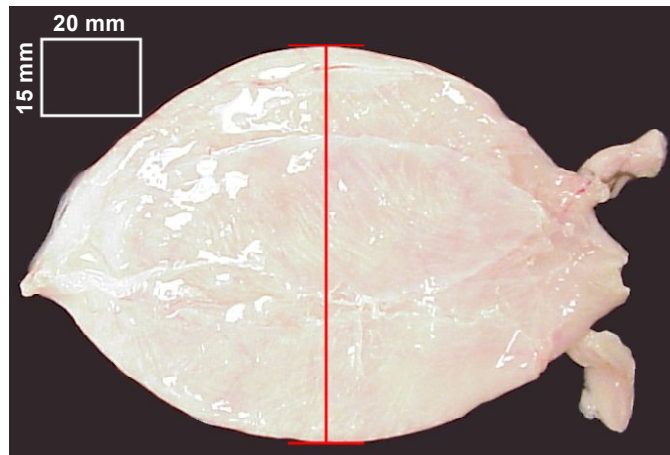


Figure 2

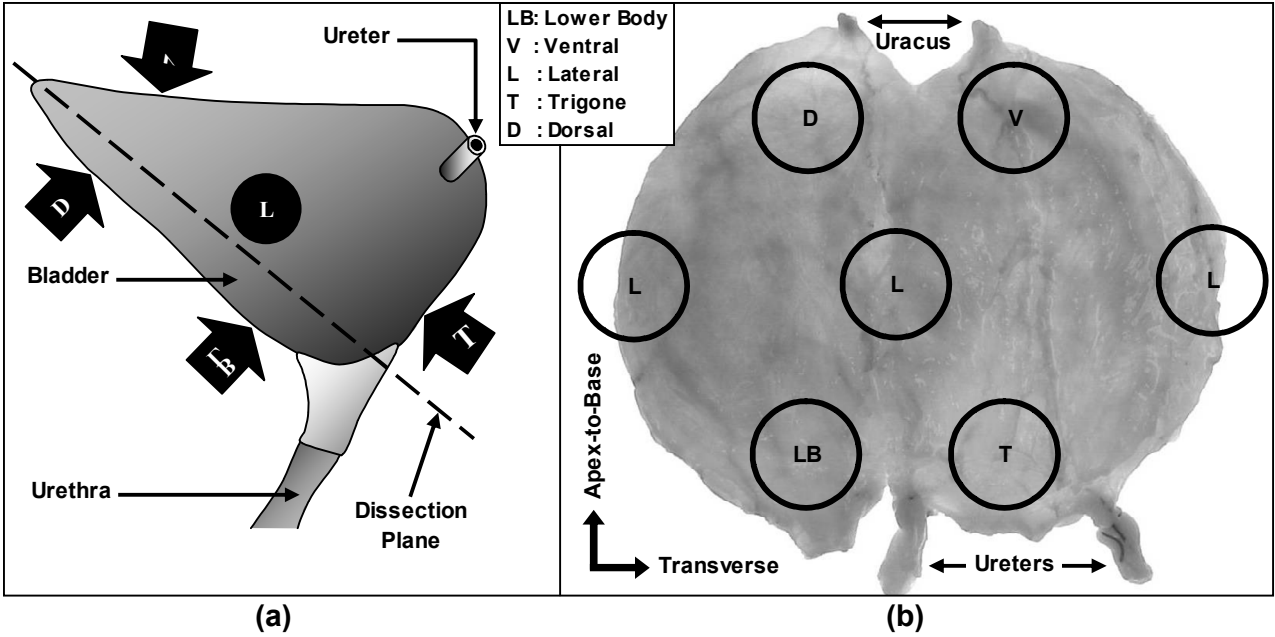


Figure 3

Figure 3

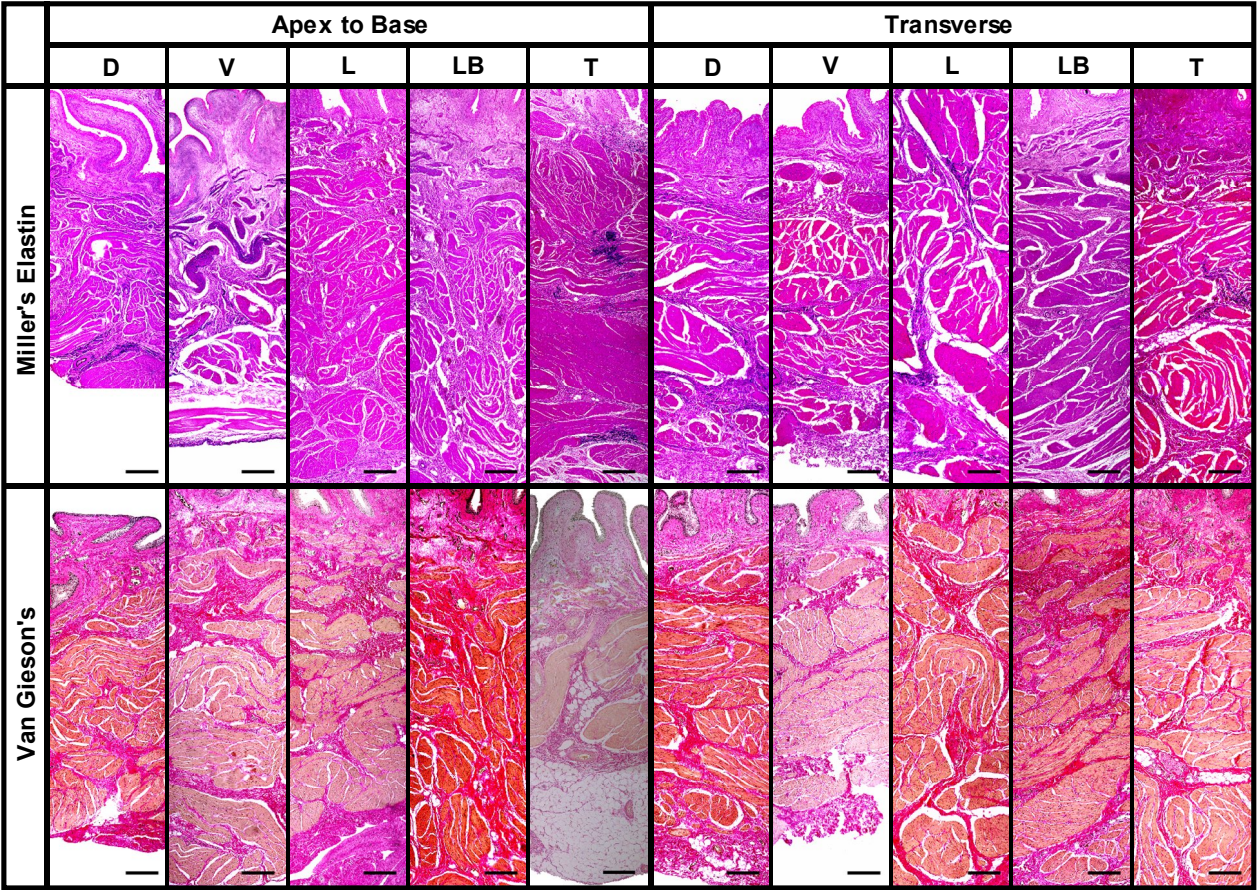




Figure 4

Figure 4

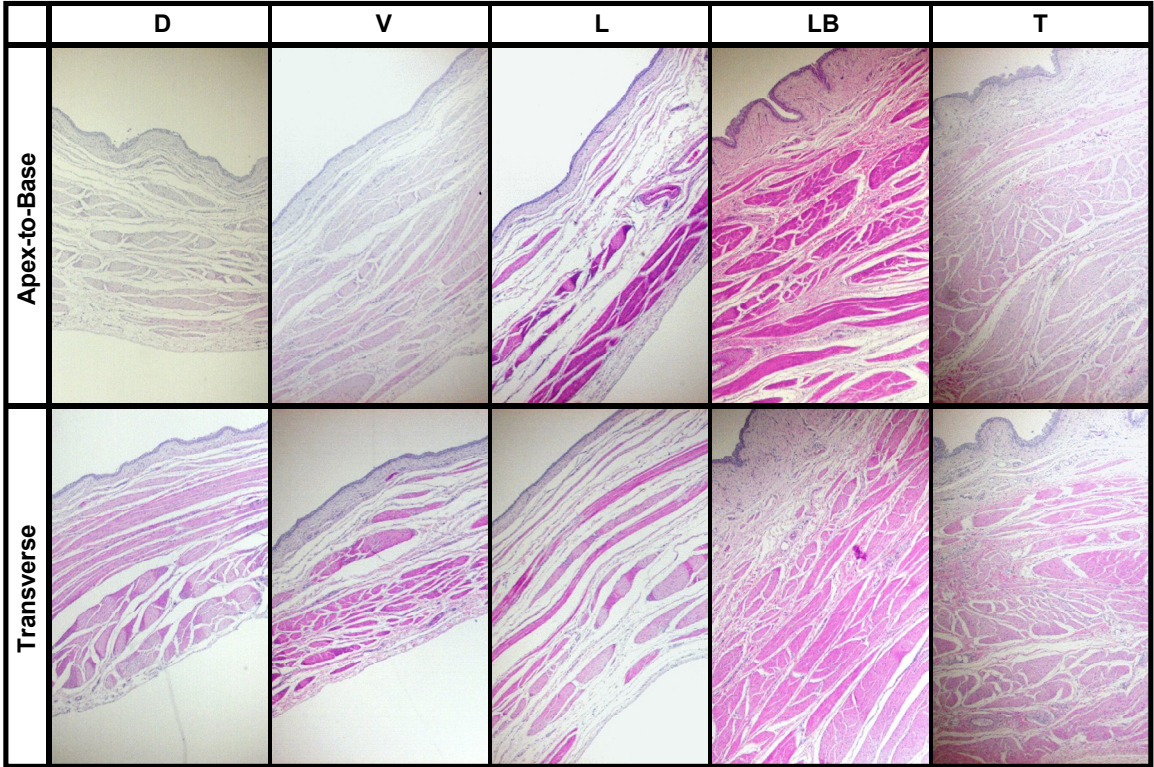




Figure 5

Figure 5

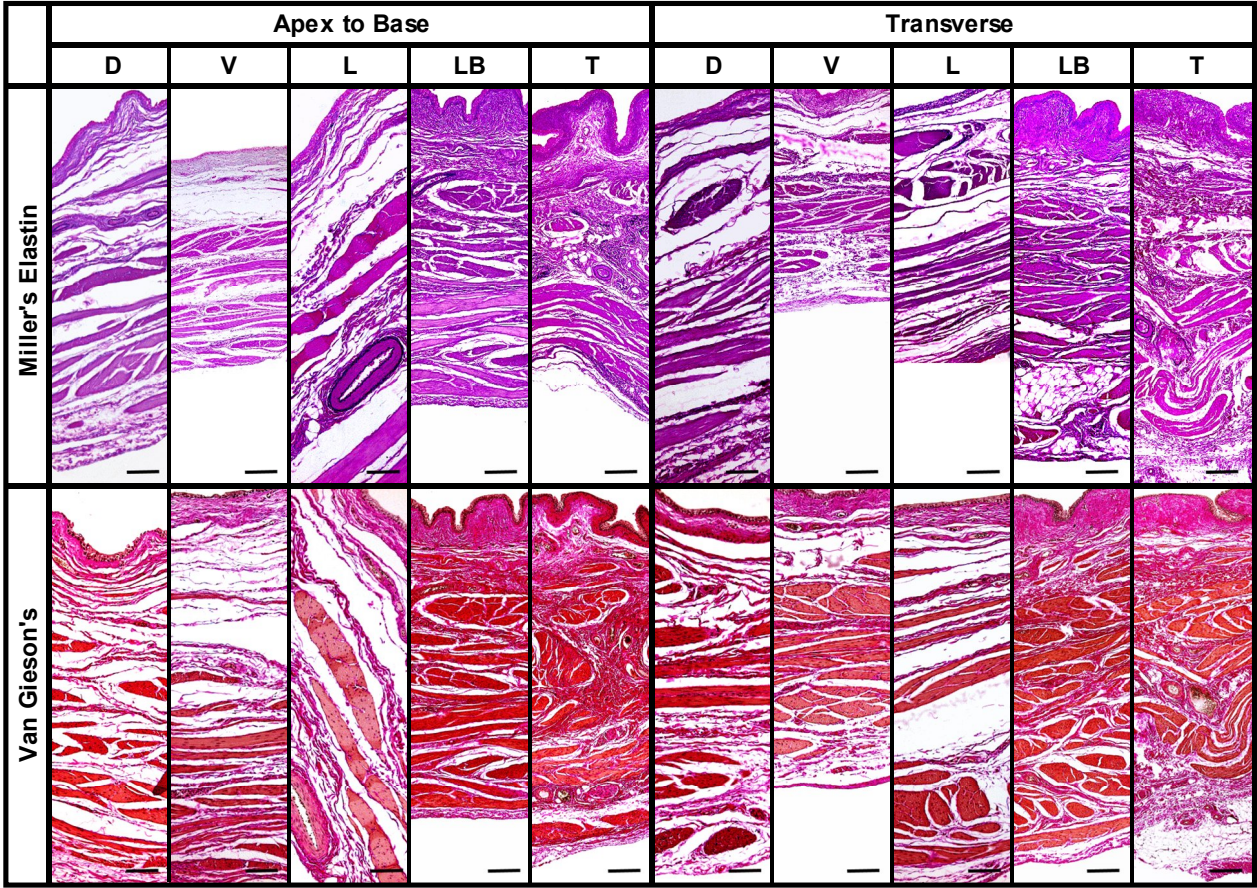


Figure 6

Figure 6

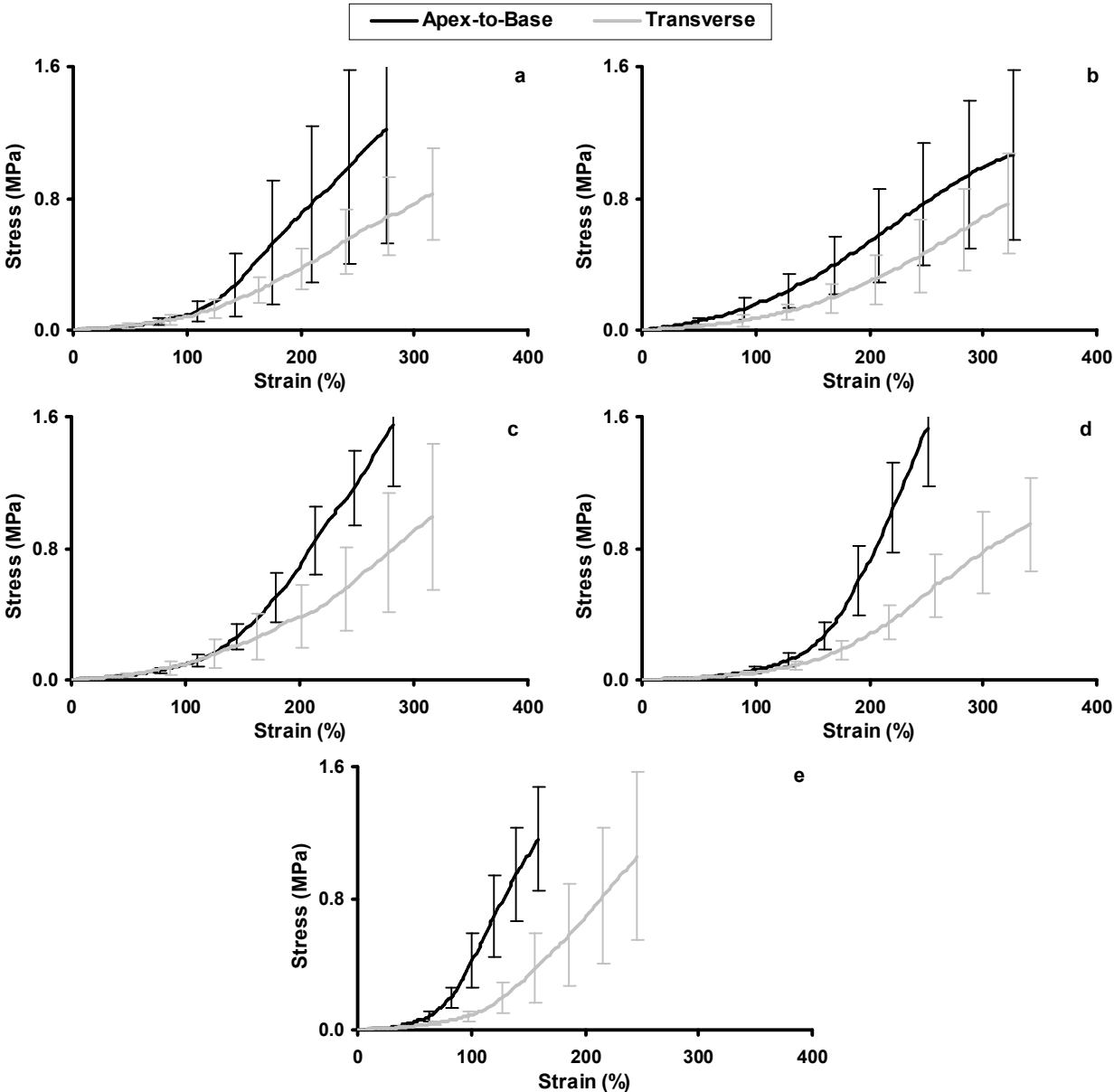


Figure 7

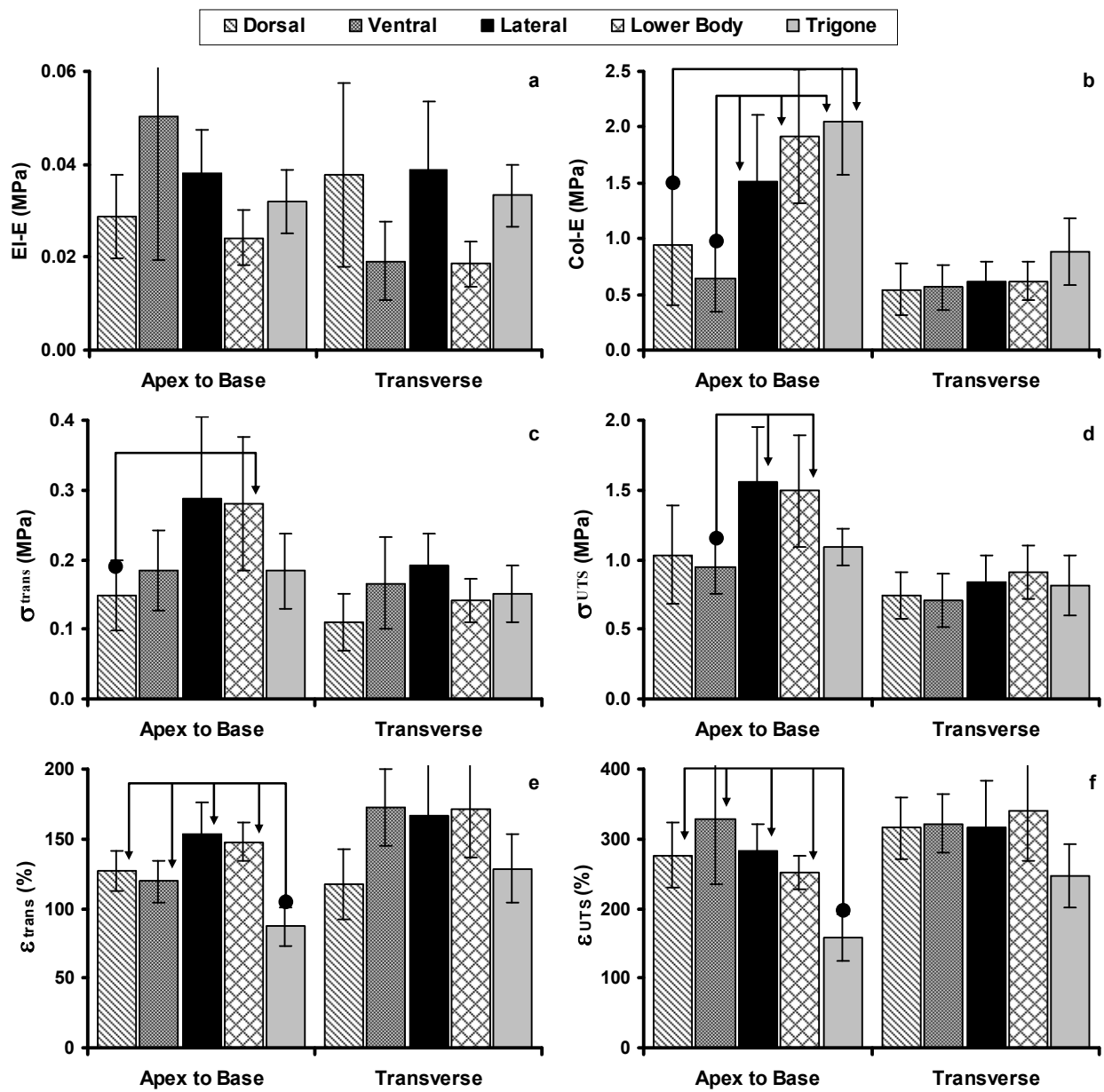
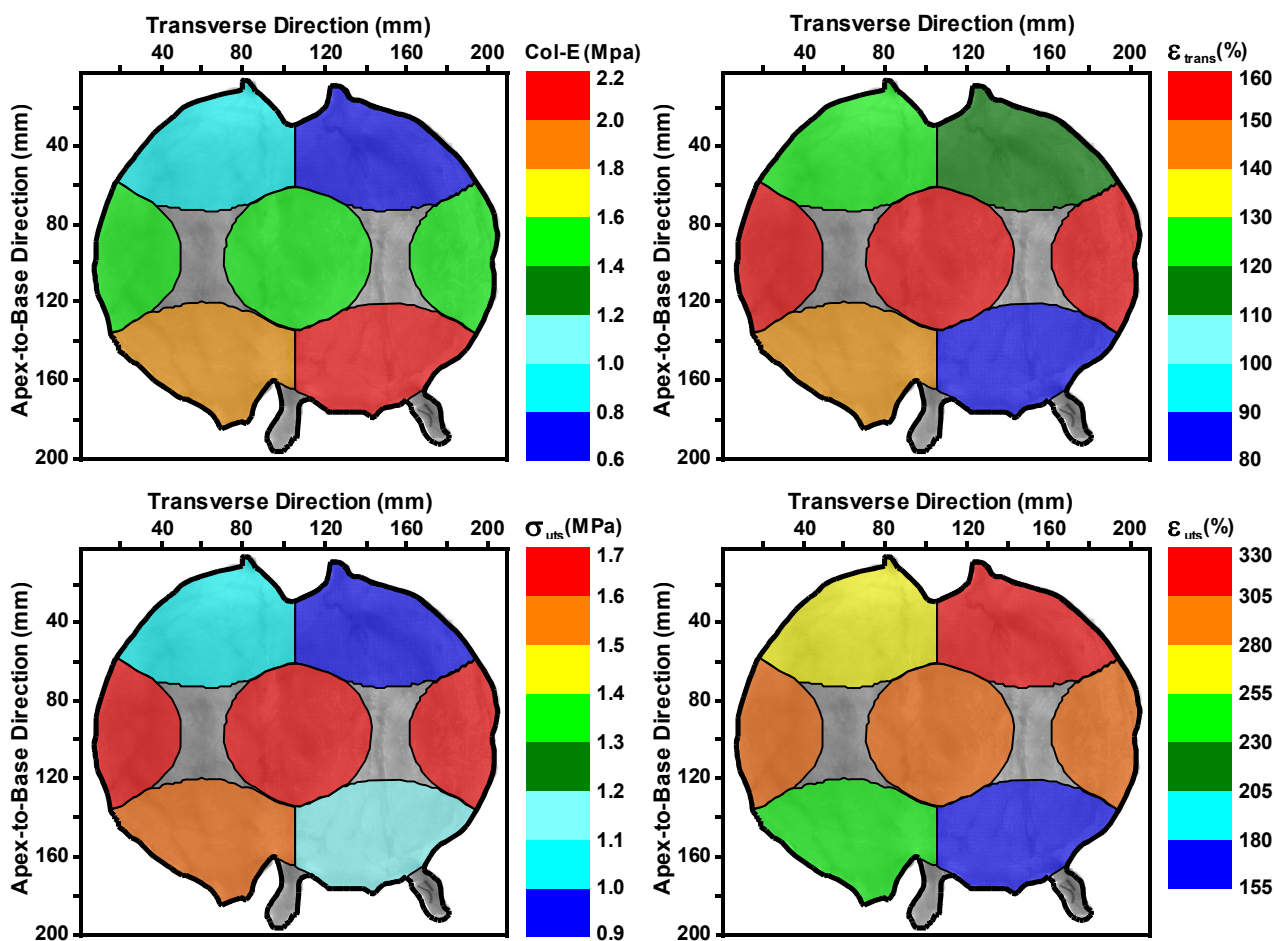


Figure 8

Figure 8



### Figure 9

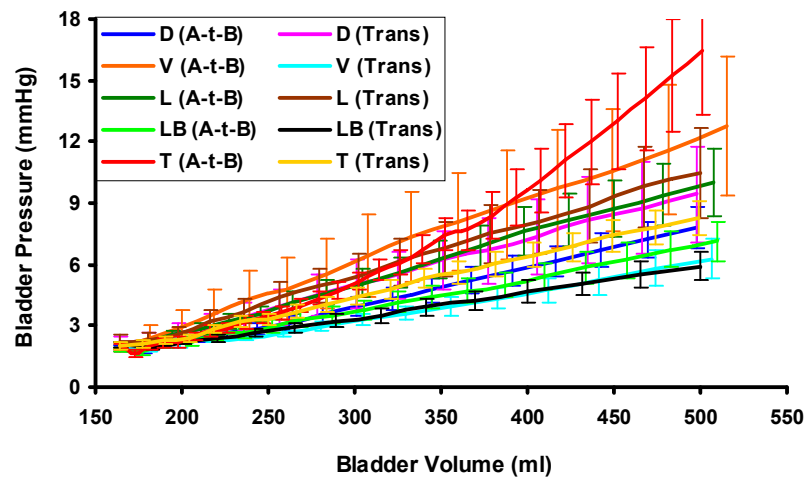
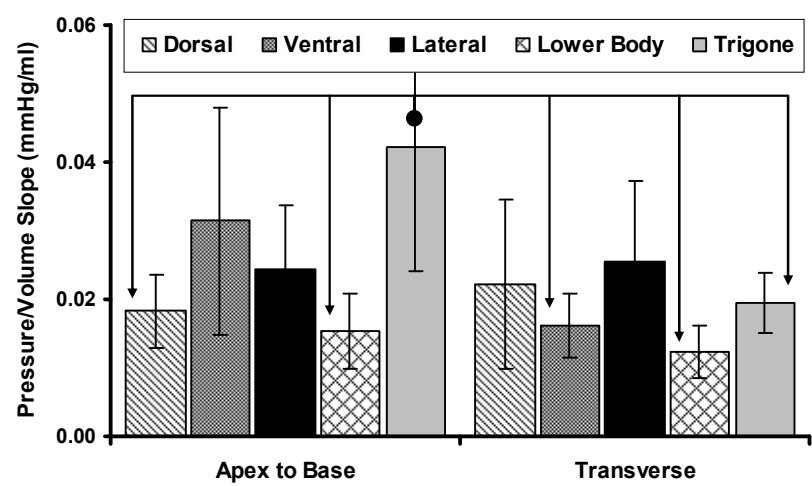


Figure 10

Figure 10



## Figure Captions

Figure 1: Bladder sizing. Bladder width was measured along the transverse line.

Figure 2: Bladder dissection and sample localization. (a) Schematic of bladder in the anterior-posterior plane; (b) Cut-opened porcine bladder showing the anatomical map of the five anatomical regions investigated

Figure 3: Staining of full thickness samples retrieved from the dorsal (D), ventral (V), lateral (L), lower body (LB) and trigone (T) regions of non-distended bladder (luminal side up). Bar: 250  $\mu\text{m}$ .

Figure 4: H & E staining of full thickness samples retrieved from the dorsal (D), ventral (V), lateral (L), lower body (LB) and trigone (T) regions of distended bladder (4 $\times$  magnification).

Figure 5: Staining of full thickness samples retrieved from the dorsal (D), ventral (V), lateral (L), lower body (LB) and trigone (T) regions of distended bladder. Bar: 250  $\mu\text{m}$ .

Figure 6: Regional mean stress-strain behaviour of the bladder wall along the apex-to-base and transverse directions (error bars indicate the 95% confidence intervals,  $n = 6$ ): a) dorsal; b) ventral; c) lateral; d) lower body; e) trigone.

Figure 7: Regional mean biomechanical parameters of the bladder wall along the apex-to-base and transverse directions (error bars indicate the 95% confidence intervals,  $n = 6$ ): a) elastin phase slope (EI-E); b) collagen phase slope (Col-E); c) transition stress ( $\sigma_{\text{trans}}$ ); d) ultimate tensile strength ( $\sigma_{\text{uts}}$ ); e) transition strain ( $\epsilon_{\text{trans}}$ ); f) failure strain ( $\epsilon_{\text{uts}}$ ). Connectors indicate significant ( $p < 0.05$ ) regional difference between originator column and end arrow column.

Figure 8: Regional topographic map of the urinary bladder showing the variation of the mean collagen phase slope (Col-E), ultimate tensile strength ( $\sigma_{\text{uts}}$ ), transition strain ( $\epsilon_{\text{trans}}$ ), and failure strain ( $\epsilon_{\text{uts}}$ ) over the five anatomical regions investigated, and along the apex-to-base direction. These results correspond to the results presented in Figure 6.

Figure 9: Mean pressure-volume profiles calculated from the stress-strain behaviour of the dorsal (D), ventral (V), lateral (L), lower body (LB), and trigone (T) bladder regions along the apex-to-base and transverse directions (mean  $\pm$  95% confidence interval,  $n = 6$ ).

Figure 10: Average slopes of the pressure-volume profiles for the dorsal, ventral, lateral, lower body, and trigone models (error bars indicate the 95% confidence intervals,  $n = 6$ ). Connectors indicate significant difference.

Table 1

Ratios of Col-E between the apex-to-base and transverse direction groups.

<b>Bladder Region:</b>	Dorsal	Ventral	Lateral	Lower Body	Trigone
<b>Col-E Ratio</b>	: 1.4	1.2	2.5	3.1	2.5